The Lorentzian approximation of ($B15b$) needed in § 4 is

$$\Phi_1(x) \simeq (1+9x^2/16)^{-1}. \qquad (B16)$$

For $\sigma_2(\Gamma_2)$ the same expressions are obtained with ρ_1 in place of ρ_2.

APPENDIX C
Transformation of the ellipsoid into a sphere of unit radius

Remember here some mathematical relations used above (see also Becker & Coppens, 1975). If the equation of an ellipsoidal surface in the system ($\mathbf{c}_i$) of its principal axes is $\sum_i z_i^2/r_i^2 = 1$ and the transformation $z_i = r_i z_i'$ is performed then this equation become $\sum_i z_i'^2 = 1$, which represents a sphere of unit radius. By this transformation any unit vector $\mathbf{u} = \sum_i u_i \mathbf{c}_i$ is transformed into the vector $\mathbf{U}' = \sum_i U_i' \mathbf{c}_i = \sum_i u_i \mathbf{c}_i / r_i$. If one denotes by ρ_u the ellipsoid radius along the vector $\mathbf{u}$, then the vector $\rho_u \mathbf{u}$ is transformed into $\mathbf{u}' = \rho_u \mathbf{U}'$ of unit length. In consequence we can write

$$1/\rho_u^2 = \sum_i u_i^2/r_i^2. \qquad (C1)$$

Now, if $\mathbf{u}$ and $\mathbf{v}$ are a pair of unit vectors whose mutual angle is φ, after transformation this angle becomes

$$\cos \varphi' = \mathbf{u}' \cdot \mathbf{v}' = \rho_u \rho_v \sum_i u_i v_i / r_i^2. \qquad (C2)$$

Finally, if t is a segment in the $\mathbf{u}$ direction, the vector $t\mathbf{u}$ is transformed into $t\mathbf{U}' = t|\mathbf{U}'|\mathbf{u}' = t'\mathbf{u}'$. Then the transformation t' of t is

$$t' = t/\rho_u. \qquad (C3)$$

References

BECKER, P. J. (1977). *Acta Cryst.* **A33**, 243-294.
BECKER, P. J. & COPPENS, P. (1974*a*). *Acta Cryst.* **A30**, 129-147.
BECKER, P. J. & COPPENS, P. (1974*b*). *Acta Cryst.* **A30**, 148-153.
BECKER, P. J. & COPPENS, P. (1975). *Acta Cryst.* **A31**, 417-425.
COPPENS, P. & HAMILTON, W. C. (1970). *Acta Cryst.* **A26**, 71-83.
DARWIN, C. G. (1922). *Philos. Mag.* **43**, 800-824.
HAMILTON, W. C. (1957). *Acta Cryst.* **10**, 629-634.
HARADA, J., MIYATAKE, H. & SAKATA, M. (1984). *Acta Cryst.* **A40**, C357.
HUTTON, J., NELMES, R. J. & SCHEEL, H. J. (1981). *Acta Cryst.* **A37**, 916-920.
KATO, N. (1976*a*). *Acta Cryst.* **A32**, 453-457.
KATO, N. (1976*b*). *Acta Cryst.* **A32**, 458-466.
KATO, N. (1979). *Acta Cryst.* **A35**, 9-16.
KATO, N. (1980). *Acta Cryst.* **A36**, 763-769.
KAWAMURA, T. & KATO, N. (1983). *Acta Cryst.* **A39**, 305-310.
NELMES, R. J. (1980). *Acta Cryst.* **A36**, 641-653.
POPA, N. C. (1976). *Acta Cryst.* **A32**, 635-641.
SEARS, V. F. (1975). *Adv. Phys.* **24**, 1-45.
SEARS, V. F. (1978). *Can. J. Phys.* **56**, 1261-1288.
SUORTTI, P. (1982). *Acta Cryst.* **A38**, 642-647.
TOMIYOSHI, S., YAMADA, M. & WATANABE, H. (1980). *Acta Cryst.* **A36**, 600-604.
VINEYARD, G. H. (1954). *Phys. Rev.* **96**, 93-98.
WERNER, S. A. (1974). *J. Appl. Phys.* **45**, 3246-3254.
ZACHARIASEN, W. H. (1967). *Acta Cryst.* **23**, 558-564.

Acta Cryst. (1987). **A43**, 316-321

X-ray Diffraction by a Low-Angle Twist Boundary Perpendicular to Crystal Surface. I. Superstructure Factor of Screw Dislocation Superlattice

BY D. M. VARDANYAN

Department of Physics, Yerevan State University, Mravyan str. 1, 375049 *Yerevan, Armenia, USSR*

AND H. M. PETROSYAN

Department of Physics, Yerevan Pedagogical Institute, Khandjyan str. 5, 375010 *Yerevan, Armenia, USSR*

(*Received* 12 *August* 1985; *accepted* 21 *October* 1986)

Abstract

The X-ray two-wave diffraction on a dislocation wall perpendicular to a crystal surface, consisting of periodically arranged dislocations (low-angle twist boundary), is considered in the case when the dislocation superlattice period is much less than the crystal extinction length. The formula obtained for the reflected intensity is of the same form as that for an ideal crystal with a modified crystal structure factor. The superstructure factor of a dislocation superlattice is calculated. The recurrence relations are produced which enable a superstructure factor to be calculated for a satellite of any order and magnitude **hb** (**h** is the diffraction vector, **b** is the Burgers vector).

1. Introduction

The grain boundary (GB) is a surface between two misorientated single crystals. The dislocation structure of a GB is well known (Hirth & Lothe, 1968;

0108-7673/87/030316-06$01.50

McLean, 1957). According to the existing model a pure twist boundary is formed by a net of two mutually perpendicular arrays of screw dislocations and is a two-dimensional superlattice (SL). A pure tilt boundary is formed by a periodic array of edge dislocations and is a one-dimensional SL. The dislocation SL period at small disorientation angles is defined as

$$z_0 \simeq b/\Delta\theta \tag{1}$$

where b is the Burgers vector modulus and $\Delta\theta$ the angle of block misorientation. When $\Delta\theta < 10°$ the boundary is called a low-angle type and when $\Delta\theta > 10°$ a high-angle type. Only the low-angle boundary is well described by the dislocation model since at larger disorientation angles, when the distance between dislocations becomes of the order of a few b, the dislocation cores deform. Low-angle GBs are formed by crystal growth, plastic strain, polygonization, epitaxial growth *etc.*

The structure of GBs has been studied by electron microscopy [for a review see Amelinckx & Dekeyser (1959)]. If the pure twist or tilt boundary plane is parallel to the foil surface then the boundary image is a net or an array of dark lines, so that each line is identified with the individual dislocation image (Schober & Balluffi, 1969). This is a direct image of the GB. Thölen (1970), by numerical integration of the Howie–Whelan equations, has shown that when the dislocation SL period is less than 0·3 of an extinction length, then the net pattern is indistinguishable from the moiré pattern. High-resolution electron microscopy was used to study [011] low-angle tilt boundaries in Ge (Bourret & Desseaux, 1979) and Al (Penisson & Bourret, 1979). For the study of the periodic structure of a GB, when the microscope image has small periodicity, diffraction techniques are useful [for a review see Sass (1980)].

When an X-ray or electron wave is diffracted by a crystal a modulated wave with a period much exceeding the lattice parameter arises in the crystal, and a GB with a periodic structure serves as a diffraction grating for this modulated wave. As a result of such a diffraction, some satellites appear on X-ray and electron diffraction patterns in the vicinity of the main Bragg reflections.

First, Spyridelis, Delavignette & Amelinckx (1967) and then Balluffi, Sass & Schober (1972) have pointed out that the GB dislocation network acts as a diffraction grating. In the last decade electron and X-ray diffraction have been successfully used (a) to detect the periodic structure of low- and high-angle GBs (Sass, Tan & Balluffi, 1975; Carter, Donald & Sass, 1979; Carter, Föll, Ast & Sass, 1981), (b) to study the relaxation effects in the GB (Erlings & Schapink, 1979), (c) to estimate the GB thickness (Budai, Gaudig & Sass, 1979; Carter, Donald & Sass, 1980), and (d) to study the detailed atomic structure of GBs (Guan & Sass, 1973, 1979; Gaudig & Sass, 1979; Budai & Sass, 1982).

In the present work the two-wave X-ray diffraction by a crystal containing a pure twist boundary perpendicular to the crystal surface is examined in the case when the dislocation SL period is much less than the crystal extinction length. In such a geometry the displacement function $\mathbf{u}(\mathbf{r})$ varies periodically with crystal depth, and falls off rapidly from both sides of the boundary. Also, the general approach to two-wave X-ray diffraction by a one-dimensional SL (Vardanyan, Manoukyan & Petrosyan, 1985) is briefly presented. Absorption is not taken into account.

The obtained formulae are analyzed in paper II (Vardanyan & Petrosyan, 1987), where the twist boundary image plane-wave profiles are plotted as well. In paper III (in preparation), the formulae for the integrated intensities are obtained.

2. General approach

The characteristic features of X-ray diffraction by a SL is the presence of satellites around the principal maxima in X-ray diffraction patterns. At $z_0 \ll \bar{\Lambda}$ (z_0 is the SL period and $\bar{\Lambda}$ the mean extinction length), the SL diffraction maxima directions are defined by

$$\bar{s}_m = m/z_0;\ m = 0, \pm 1, \dots, \tag{2}$$

where $\bar{s}$ is the average over the SL period value of the local deviation $s(z)$ from the Bragg condition:

$$\bar{s} = z_0^{-1} \int\limits_0^{z_0} s(z)\,\mathrm{d}z.$$

Since

$$s(z) = s + \mathrm{d}(\mathbf{hu})/\mathrm{d}z, \tag{3}$$

then

$$\bar{s} = s + z_0^{-1}[\mathbf{hu}(z_0) - \mathbf{hu}(0)], \tag{4}$$

where $\mathbf{h}$ is the diffraction vector, $\mathbf{u}(z)$ is the displacement field, and

$$s = h(\theta - \theta_B) \tag{5}$$

indicates the deviation from the Bragg condition in the case of an ideal crystal. At $z_0 \ll \bar{\Lambda}$ within the limits of the mth satellite one may consider the SL as an ideal crystal with the modified structure factor

$$F_{hm} = |M_m| F_h, \tag{6}$$

where M_m may be called the superstructure factor:

$$M_m = z_0^{-1} \int\limits_0^{z_0} \mathrm{d}z \exp\left[2\pi i(hu) + 2\pi i s_m z\right] \tag{7}$$

and

$$s_m = z_0^{-1}\{m - [\mathbf{hu}(z_0) - \mathbf{hu}(0)]\}. \tag{8}$$

The superstructure factor is the Fourier component of the function

$$\exp\{2\pi i(\mathbf{hu}) - 2\pi i[\mathbf{hu}(z) - \mathbf{hu}(0)]zz_0^{-1}\},$$

so that

$$|M_m| \leq 1 \quad \text{and} \quad \sum_{m=-\infty}^{\infty} |M_m|^2 = 1, \tag{9}$$

as follows from the Parseval theorem. In this approximation the angular separation of the adjacent satellites is constant,

$$\Delta = z_0^{-1}. \tag{10}$$

Equation (7) suggests that the amplitude of a reflected wave from a SL cell is calculated in the kinematical approximation. Taking advantage of the dynamical expression for the ideal nonabsorbing crystal reflectance (James, 1948) and taking into account (6), within the mth satellite limits, for the SL reflectance, one may write

$$R_m(s) = \frac{\sin^2\{\pi D \Lambda_m^{-1}[1 + \Lambda_m^2(s - s_m)^2]^{1/2}\}}{1 + \Lambda_m^2(s - s_m)^2}, \tag{11}$$

where

$$\Lambda_m = \bar{\Lambda}/|M_m| \tag{12}$$

is the SL extinction length of the mth satellite, and D is the crystal thickness.

From (1), the condition $z_0 \ll \bar{\Lambda}$ can be written as

$$\Delta\theta \gg b\bar{\Lambda}^{-1}. \tag{13}$$

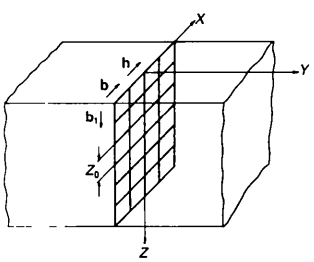

Fig. 1. Screw dislocation net on two-crystal interface. Diffraction planes correspond to $y = \text{constant}$; **b** and $\mathbf{b}_1$ are the Burgers vectors.

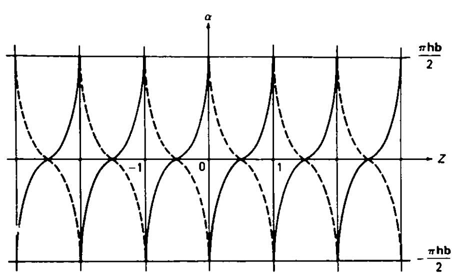

Fig. 2. The $\alpha(Z)$ dependence. Solid lines correspond to $y > 0$ and dashed lines to $y < 0$.

For X-rays, $\bar{\Lambda}$ is of the order 5-50 μm so the condition (13) means that $\Delta\theta \gg 10^{-4}$-10^{-5} rad. Thus, the present theory is valid if $10^{-4} < \Delta\theta < 10^{-1}$ rad.

3. Twist boundary displacement field

Consider a set of two crystal blocks with the lattices turned with respect to each other by an angle $\Delta\theta$ as shown in Fig. 1. The GB is of a twist type, and according to the dislocation model is composed of a net of two mutually perpendicular arrays of screw dislocations, so that in a given array the dislocations have the same Burgers vectors. The diffraction planes are those with $y = \text{constant}$. Since $(\mathbf{hb}_1) = 0$, the array of dislocations perpendicular to the surface is invisible.

The displacement field of the jth screw dislocation in an infinite medium is of the form (Hirth & Lothe, 1968)

$$\begin{aligned} u_{xj} &= (2\pi)^{-1} b \arctan[(z + jz_0)y^{-1}] \\ u_{yj} &= u_{zj} = 0. \end{aligned} \tag{14}$$

In the present work the surface relaxation effect is neglected. Summing the single dislocation contributions, for the phase term $\alpha = 2\pi(\mathbf{hu})$ of a dislocation wall we get (Proudnikov, Brychkov & Marichev, 1981)

$$\begin{aligned} \alpha &= 2\pi h \sum_{j=-\infty}^{\infty} u_{xj} \\ &= -n \arctan[\tanh(\pi|Y|)\cot(\pi Z)], \end{aligned} \tag{15}$$

where

$$Y = y/z_0; \qquad Z = z/z_0 \tag{16}$$

are the normalized coordinates and

$$n = (\mathbf{hb}) \operatorname{sign} y. \tag{17}$$

An analogous expression was obtained by Thölen (1970) in the case when the boundary is parallel to the crystal surface. The plot of the periodic function $\alpha(Z)$ is shown in Fig. 2.

As seen from (13), the boundary plane $y = 0$ is a SL of stacking faults with the phase factor πn.*

On both sides of the boundary the $\alpha(Z)$ period remains constant, but the strain amplitude exponentially decreases, so the effective thickness of the dislocation wall is of the order of the SL period. Thus, the displacement field of the dislocation wall is a short-range one, since the single dislocation contributions partially compensate each other. Far from the boundary the phase term within the SL period is

* It should be noted that the X-ray diffraction by SL of stacking faults is considered by Vardanyan & Manoukyan (1982, 1983) in the Bragg case and Vardanyan & Manoukyan (1985) in the Laue case, without the restriction $z_0 \ll \bar{\Lambda}$.

linear with Z:

$$\alpha(Z) = \pi n(Z - l_1 - \tfrac{1}{2}), \tag{18}$$

where l_1 is an integer and $l_1 < Z < l_1 + 1$.

Expression (18) means that the blocks are turned with respect to each other by the angle

$$\Delta\theta = (\pi h z_0)^{-1}\,\mathrm{d}\alpha/\mathrm{d}Z = b/z_0$$

in accordance with (1).

4. The dislocation SL superstructure factor

Substituting (15) into (8), we find the diffraction maxima directions

$$s_l = z_0^{-1}(m - n/2) = l/2z_0, \tag{19}$$

where $l = 2m - n$. Since the dislocations are full ones, then n is an integer and l and n are of the same parity.

Substituting (15) and (19) into (7) and replacing the integration variable z by Z, we obtain*

$$M_{l,n} = \int_0^1 \mathrm{d}Z \exp\{-in \arctan[\tanh(\pi|Y|)\cot(\pi Z)] + i\pi l Z\}. \tag{20}$$

In Appendix A two useful relations are derived:

$$M_{l,n} = (-1)^l M_{-l,-n}, \tag{21}$$

$$lM_{l,n} - nM_{n,l} = 0, \tag{22}$$

which enable one to restrict the consideration to values of $l \geq n$. The integral (20) is calculated in Appendix A and has the form

$$M_{l,n} = (-i)^n \frac{\Gamma(l/2)q^{(l-n)/4}}{\Gamma(n/2)\Gamma[(l-n/2)+1]} \times F\left(-\frac{n}{2}, \frac{l}{2}; \frac{l-n}{2}+1; q\right), \tag{23}$$

where

$$q = \exp(-4\pi|Y|), \tag{24}$$

$\Gamma(x)$ is the gamma function and $F(a, b; c; x)$ the Gauss hypergeometric function.

At $l \leq n$, $M_{l,n}$ may be calculated from (22) and (23). Using the general formula (23), we get:

(a) at $l = 0$,

$$M_{0,n} = q^{|n|/4}; \tag{25a}$$

(b) at $l = 2k > 0$ and $n = 2r > 0$,

$$M_{2k,2r} = (-1)^r(1-q)q^{(k-r)/2}P_{r-1}^{(k-r,1)}(1-2q); \tag{25b}$$

(c) at $l = 2k > 0$ and $n = -2r < 0$,

$$M_{2k,-2r} = 0; \tag{25c}$$

(d) at $l = 2k-1$ and $n = 2r-1 > 0$,

$$M_{2k-1,2r-1} = -i\frac{\Gamma(k-\frac{1}{2})q^{(k-r)/2}}{\Gamma(r-\frac{1}{2})\Gamma(k-r+1)} \times F(-r+\tfrac{1}{2}, k-\tfrac{1}{2}; -r+k+1; q); \tag{25d}$$

(e) at $l = 2k-1 > 0$ and $n = 1-2r < 0$,

$$M_{2k-1,1-2r} = -i\pi^{-1}\frac{\Gamma(k-\frac{1}{2})\Gamma(r+\frac{1}{2})}{\Gamma(k+r)} q^{(k+r-1)/2} \times F(r-\tfrac{1}{2}, k-\tfrac{1}{2}; k+r; q); \tag{25e}$$

where $P_n^{(\alpha,\beta)}(x)$ are the Jacobi polynomials, k and r are positive integers.

In Appendix A the other representation of $M_{l,n}$ are given.

It should be noted that (25) are not convenient for computation of $M_{l,n}$ at large l and n. Therefore, in Appendix B we suggest a rational technique for $M_{l,n}$ computation based on recurrence relations.

APPENDIX A

Evaluation of the integral (20)

To integrate the expression

$$M_{l,n} = \int_0^1 \mathrm{d}Z \exp\{-in \arctan[\tanh(\pi|Y|)\cot(\pi Z)] + i\pi l Z\} \tag{A1}$$

we make use of the relation

$$\arctan u = -(i/2)\ln[(1+iu)/(1-iu)],$$

which reduces (A1) to the form

$$M_{l,n} = \int_0^1 [\sin\pi(Z+i|Y|)]^{n/2}[\sin\pi(Z-i|Y|)]^{-n/2} \times \exp(i\pi l Z). \tag{A2}$$

The substitution of

$$w = q^{-1/2}\exp(2\pi i Z), \tag{A3}$$

where

$$q = \exp(-4\pi|Y|), \tag{A4}$$

transforms (A2) into an integral on the w complex plane:

$$M_{l,n} = (2\pi i)^{-1}q^{(l-n)/4}\int_C (1-qw)^{n/2} \times (1-w)^{-n/2}w^{-1+l/2}\,\mathrm{d}w, \tag{A5}$$

where the contour C is a circle of radius $q^{-1/2}$ (Fig. 3).

We show that the following relation holds:

$$lM_{l,n} - nM_{n,l} = 0. \tag{A6}$$

To do that we integrate (A5) by parts:

$$M_{l,n} = (2\pi i)^{-1}(n/l)q^{(l-n)/4}\int_C (1-qw)^{-1+n/2} \times (1-w)^{1-n/2}w^{l/2}\,\mathrm{d}[(1-qw)/(1-w)],$$

* Hereafter we write $M_{l,n}$ instead of M_l. The first subscript indicates the diffraction maximum number, the second one being the value of **hb** sign y.

and making the substitution of variable

$$u=(1-qw)(1-w)^{-1}q^{-1},$$

which maps the contour C onto itself, we obtain

$$M_{l,n}=-(2\pi i)^{-1}(n/l)q^{(n-l)/4}\int_C(1-qu)^{l/2}$$
$$\times(1-u)^{-l/2}u^{-1+n/2}\,du$$

whence ($A6$) follows.

The substitution of the variable Z by $(1-Z)$ in ($A1$) leads to the following relation:

$$M_{l,n}=(-1)^l M_{-l,-n}. \qquad (A7)$$

At an even positive n the integrand in ($A5$) has the first-order pole $w_1=0$ at $l=0$ and the pole of order $|n|/2$ with $w_2=q^{-1}$. Since $q<1$, then w_2 is beyond the circle of radius $q^{-1/2}$ and does not contribute to the integral. Therefore, for such n and $l>0$ we get $M_{l,n}=0$.

The integral ($A5$) is expressed in terms of the Gauss hypergeometric function (Bateman & Erdelyi, 1953):

$$F(a,b;c;x)=1+\frac{ab}{c}x+\frac{a(a+1)b(b+1)}{1\times2\times c(c+1)}x^2+\ldots$$

and at $l\geq n$ has the form

$$M_{l,n}=(-i)^n\frac{\Gamma(l/2)}{\Gamma(n/2)\Gamma[1+(l-n)/2]}$$
$$\times q^{l-n/4}F\left(-\frac{n}{2},\frac{l}{2};1+\frac{(l-n)}{2};q\right). \qquad (A8)$$

From ($A6$) and ($A8$) at $l\leq n$ we have

$$M_{l,n}=(-i)^l\frac{\Gamma(n/2+1)q^{(n-l)/4}}{\Gamma(l/2+1)\Gamma[1+(n-l)/2]}$$
$$\times F\left(-\frac{l}{2},\frac{n}{2};\frac{n-l}{2}+1;q\right). \qquad (A9)$$

At $l=0$, from ($A9$) we get

$$M_{0,n}=q^{|n|/4}. \qquad (A10)$$

At $l=2k>0$ and $n=2r>0$ the hypergeometric series is cut off, and from ($A8$) we get

$$M_{2k,2r}=(-1)^r q^{(k-r)/2}(1-q)P_{r-1}^{(k-r,1)}(1-2q) \qquad (A11a)$$
$$=q^{(k-r)/2}(q-1)\sum_{i=0}^{r-1}(-1)^i\binom{k-1}{i}\binom{r}{r-1-i}$$
$$\times(1-q)^i q^{r-1-i} \qquad (A11b)$$

where $P_n^{(\alpha,\beta)}(x)$ are the Jacobi polynomials and $\binom{m}{n}$ are the binomial coefficients.

At $l=2k>0$ and $n=-2r<0$ we obtain

$$M_{2k,-2r}=0 \qquad (A12)$$

since $[\Gamma(-r)]^{-1}=0$.

At $l=2k-1>0$ and $n=2r-1>0$, we find

$$M_{2k-1,2r-1}=-i\frac{\Gamma(k-\frac{1}{2})}{\Gamma(r-\frac{1}{2})\Gamma(k-r+1)}q^{(k-r)/2}$$
$$\times F(-r+\tfrac{1}{2},k-\tfrac{1}{2};k-r+1;q) \qquad (A13a)$$
$$=-i\frac{q^{(r-k)/2}(1-q)^{1/2}}{\Gamma(r-\frac{1}{2})\Gamma(k+\frac{1}{2})}$$
$$\times\frac{d^{r-1}}{dq^{r-1}}[q^{k-1}(1-q)^{r-1}B_{k-1}]. \qquad (A13b)$$

At $l=2k-1>0$ and $n=1-2r<0$,

$$M_{2k-1,1-2r}=-i\frac{\Gamma(k-\frac{1}{2})\Gamma(r+\frac{1}{2})}{\pi\Gamma(k+r)}q^{(k+r-1)/2}$$
$$\times F(r-\tfrac{1}{2},k-\tfrac{1}{2};k+r;q) \qquad (A14a)$$
$$=-i\frac{2q^{(k+r-1)/2}(1-q)^{3/2}}{\Gamma(r-\frac{1}{2})\Gamma(k+\frac{1}{2})}$$
$$\times\frac{d^r}{dq^r}[(1-q)^{r-1}B_{k-1}], \qquad (A14b)$$

where

$$B_k=d^k[(1-q)^{k-1/2}E(q)]/dq^k \qquad (A15)$$

and $E(q)$ is the complete elliptic integral of the second kind (see Appendix B).

In obtaining ($A13b$) and ($A14b$) we made use of formulae for derivatives of the hypergeometric function (Abramowitz & Stegun, 1964).

APPENDIX B

Recurrence relations for $M_{l,n}$

Using the relations between functions contiguous to $F(a,b;c;x)$ (Abramowitz & Stegun, 1964), namely,

$$xb(c-a)F(a,b+1;c+1;x)$$
$$+c(c-1)F(a,b-1;c-1;x)$$
$$-c[c-1+x(b-a)]F(a,b;c;x)=0 \qquad (B1)$$

and ($A8$), for a fixed n we obtain the following recurrence relation:

$$(l+2)M_{l+2,n}+(l-2)M_{l-2,n}$$
$$-[l-n+q(l+n)]q^{-1/2}M_{l,n}=0. \qquad (B2)$$

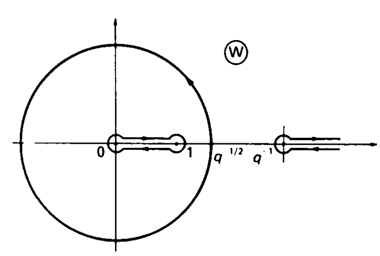

Fig. 3. The integration contour in the w plane.

For a fixed l the recurrence relation is of the form

$$nM_{l,n+2}+nM_{l,n-2}+[l-n-q(l+n)]q^{-1/2}M_{l,n}=0. \quad (B3)$$

For even l and n from ($A12$) we have $M_{l,n}=0$ if $nl<0$.

The relation ($B2$) with the initial values

$$M_{0,n}=q^{|n|/4}, \quad (B4)$$

$$M_{-2,n}=0 \quad (B5)$$

enables one to find $M_{l,n}$ for even values of l and n.

For example, at $l=2$, from ($B2$), ($B4$) and ($B5$) we have

$$M_{2,n}=\tfrac{1}{2}nq^{(n-2)/4}(q-1). \quad (B6)$$

In the same way, at $l=4$,

$$M_{4,n}=\tfrac{1}{8}n(q-1)[q(n+2)-n+2]q^{(n-4)/4}. \quad (B7)$$

For odd l and n the initial values are

$$M_{1,1}=-M_{-1,-1}=2\pi^{-1}E, \quad (B8)$$

$$M_{1,-1}=-M_{-1,1}=2\pi^{-1}q^{-1/2}[E-(1-q)K], \quad (B9)$$

where

$$K=(\pi/2)F(\tfrac{1}{2},\tfrac{1}{2};1;q)=\int\limits_0^{\pi/2}(1-q\sin^2\varphi)^{-1/2}\,\mathrm{d}\varphi$$

$$E=(\pi/2)F(-\tfrac{1}{2},\tfrac{1}{2};1;q)=\int\limits_0^{\pi/2}(1-q\sin^2\varphi)^{1/2}\,\mathrm{d}\varphi$$

are the complete elliptic integrals of the first and second kinds, respectively.

For example, using ($B2$) and ($B3$) one may obtain

$$M_{3,1}=(\tfrac{2}{3}\pi)q^{-1/2}[E(1+2q)-K(1-q)], \quad (B10)$$

$$M_{3,-1}=(\tfrac{2}{3}\pi)q^{-1}[E(2-q)-2K(1-q)]. \quad (B11)$$

The recurrence relations ($B2$) and ($B3$) are especially valuable in computing. In this case the complete elliptic integrals K and E can be approximated by polynomials (Abramowitz & Stegun, 1964). The recurrence procedure is stable if the errors do not increase. But, if the relative error increases, and it can even exceed the sought function magnitude (*e.g.* at small q), the process is unstable. In this case one may use the Miller algorithm, in which the recurrence process is carried out in the reverse direction.

References

ABRAMOWITZ, M. & STEGUN, J. A. (1964). *Handbook of Mathematical Functions.* New York: Dover.

AMELINCKX, S. & DEKEYSER, W. (1959). *Solid State Phys.* **8**, 325.

BALLUFFI, R. W., SASS, S. L. & SCHOBER, T. (1972). *Philos. Mag.* **26**, 585.

BATEMAN, H. & ERDELYI, A. (1953). *Higher Transcendental Functions.* Vol. I. New York: McGraw-Hill.

BOURRET, A. & DESSEAUX, J. (1979). *Philos. Mag.* **39**, 405–418.

BUDAI, J., GAUDIG, W. & SASS, S. L. (1979). *Philos. Mag.* **40**, 757–767.

BUDAI, J. & SASS, S. L. (1982). *J. Phys. (Paris)*, **43**, C6, 103–113.

CARTER, C. B., DONALD, A. M. & SASS, S. L. (1979). *Philos. Mag.* **39**, 533–549.

CARTER, C. B., DONALD, A. M. & SASS, S. L. (1980). *Philos. Mag.* **A41**, 467–475.

CARTER, C. B., FÖLL, H., AST, D. G. & SASS, S. L. (1981). *Philos. Mag.* **A43**, 441–467.

ERLINGS, J. G. & SCHAPINK, F. W. (1979). *Phys. Status Solidi A*, **52**, 529.

GAUDIG, W. & SASS, S. L. (1979). *Philos. Mag.* **A39**, 725–741.

GUAN, D. Y. & SASS, S. L. (1973). *Philos. Mag.* **27**, 1211–1223, 1225–1235.

GUAN, D. Y. & SASS, S. L. (1979). *Philos. Mag.* **A39**, 293–315.

HIRTH, J. P. & LOTHE, J. (1968). *Theory of Dislocations.* New York: McGraw-Hill.

JAMES, R. W. (1948). *The Optical Principles of X-ray Diffraction*, edited by SIR LAWRENCE BRAGG. London: Bell.

MCLEAN, D. (1957). *Grain Boundaries in Metals.* Oxford: Clarendon Press.

PENISSON, J. M. & BOURRET, A. (1979). *Philos. Mag.* **40**, 811–824.

PROUDNIKOV, A. P., BRYCHKOV, YU. A. & MARICHEV, O. I. (1981). *Integrals and Series.* Moscow: Nauka.

SASS, S. L. (1980). *J. Appl. Cryst.* **13**, 109–127.

SASS, S. L., TAN, T. Y. & BALLUFFI, R. W. (1975). *Philos. Mag.* **31**, 559–573.

SCHOBER, T. & BALLUFFI, R. W. (1969). *Philos. Mag.* **31**, 511–518.

SPYRIDELIS, J., DELAVIGNETTE, P. & AMELINCKX, S. (1967). *Mater. Res. Bull.* **2**, 615.

THÖLEN, A. R. (1970). *Phys. Status Solidi A*, **2**, 537–550.

VARDANYAN, D. M. & MANOUKYAN, H. M. (1982). *Phys. Status Solidi A*, **69**, 475–482.

VARDANYAN, D. M. & MANOUKYAN, H. M. (1983). *Phys. Status Solidi A*, **79**, 617–622.

VARDANYAN, D. M. & MANOUKYAN, H. M. (1985). Proc. Conf. on the Problems of X-ray Diagnostics of Crystal Imperfection, Yerevan, Armenia, USSR.

VARDANYAN, D. M., MANOUKYAN, H. M. & PETROSYAN, H. M. (1985). *Acta Cryst.* **A41**, 212–217.

VARDANYAN, D. M. & PETROSYAN, H. M. (1987). *Acta Cryst.* **A43**, 322–326.